Research reactive current detection method for STATCOM under grid-side asymmetrical faults

HONGSHENG SU[1,*], KAI CHEN[1], XIAOYAN LIANG[2]

[1]*School of Automation and Electrical Engineering, Lanzhou Jiaotong University, Lanzhou 730070, China*
[2]*Huanghua Supply Corporation, Qihai Branch, State Grid Corporation, Jianzha 811220, China*
([1,*]shsen@163.com)

Abstract: - To aim at the deficiencies of traditional $i_d - i_q$ detection method of reactive current of STATCOM that will generate detecting error under grid-side asymmetrical faults. As being in asymmetrical voltage condition, there will have a phase angle difference existing used to calculate the value of the compensation commending current between the detected voltage and its positive sequence voltage. To solve the issue, a revised $i_d - i_q$ detection method is proposed which can offer an auxiliary phase difference α between positive sequence voltage and d-axis, which offsets the detected errors, such that the control accuracy of STATCOM is improved, which is quite significant for safe operation of the wind power plant grid-connected. The simulation results show that the proposed method is effective and feasible.

Key-Words: - Doubly-fed induction generator (DFIG), STATCOM, reference compensation current

1 Introduction

In recent years, wind energy has become one of the most popular green renewable energy resources around the world due to its advantages to offer clean and abundant power [1,2]. The doubly-fed induction generator (DFIG) is the most common technology used in wind energy conversation systems which is connected to an AC network through voltage source converters [3]. Consequently it is essential to preserve the power quality standard at the interface of the grid from the destructive effects affected by wind turbine such as voltage fluctuation, switching operation, voltage dips, reactive power and grid harmonic distortion[4]. There are many reports on voltage stability under wind power plants connected to power grid that require a wind turbine to remain connected during a fault and after fault clearance [5,6]. Under the fault conditions, the grid sides can not provide sufficient reactive power and voltage support [7]. Some studies have been done in order to solve this problem, and proposed some good methods and achieved some better effects. With the development of Flexible AC transmission systems[8] (FACTS) based power electronic converters, static synchronous compensator[9] (STATCOM) is an option available to provide controlled dynamic reactive power compensation, and currently being used extensively in power systems because of its capability to provide flexible power flow control. In [10-13] the necessity to use STATCOM in DFIG-based wind farm during fault condition is stated, and which possesses some advantages compared with other compensators, say, to generate fewer harmonics, and require a much smaller reactor, and respond fast and continuously compensate lagging or leading reactive power.

For STATCOM, the generation of reference reactive current and control is critical to obtain perfect control performance. Compensation current detection method is one of the important core technologies of STATCOM, and also a key factor to effectively solve power quality questions in grid-side [14]. In recent years, there have been some experts and scholars to propose some improved reactive current detection methods for STATOM. In [15] a $p-q$ current detection method based on instantaneous reactive power theory is proposed. This method will produces detecting error when voltage is unbalance. In [16] a $i_p - i_q$ current detection method is proposed which is worked well under three-phase symmetrical systems, but in asymmetrical faults condition, the method will get into difficulties. Based on it, to detect accurately value of compensation current, this paper presents an improved $i_d - i_q$ current detection method which can correct the deviation. And according to the phase

angle between positive sequence fundamental voltage and d-axis, the value of the compensation commending current is calculated and obtained. In order to verify the mentioned method, eventually, the simulations under each condition are conducted, and prove the effectiveness of the method proposed.

2 DFIG-based Wind Turbine Electromagnetic Transient Model

The DFIG is a rotor induction generator with its stator winding connected directly to the three phase grid-side, and the rotor windings fed by the rotor side converter. And so, during grid faults, there are large current inducted in the rotor windings, and this might generate a risk of voltage instability. And sot it becomes quite important to establish a suitable electromagnetic transient equivalent model of DFIG to describe its electromagnetic transient process. The simplified single phase equivalent circuit of DFIG [17] is shown in Figure1.

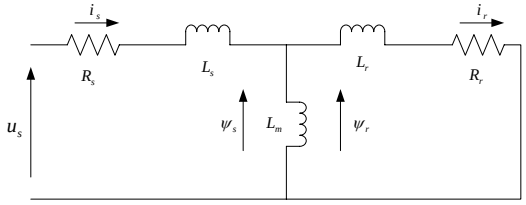

Fig.1 Simplified equivalent circuit of DFIG

where u_{s} expresses the stator voltage, and R_{s}, R_{r} represent the stator and rotor resistance, and L_{s}, L_{m}, and L_{r} represent the inductance of the stator, and the magnetic, and the rotor inductance, respectively. And ψ_{s}, and ψ_{r} represent the flux of the stator and the rotor, separately, and i_{s} and i_{r} respectively are the current of the stator and the rotor.

The voltage and flux equations of DFIG can be written by on the synchronous rotating d-q reference frame [14]

$$\begin{cases} u_{sd} = p\psi_{sd} - \omega_1\psi_{sq} + R_{\mathrm{s}}i_{sd} \\ u_{sq} = p\psi_{sq} + \omega_1\psi_{sd} + R_{\mathrm{s}}i_{sq} \\ u_{rd} = p\psi_{rd} - \omega_1\psi_{sq} + R_{\mathrm{r}}i_{rd} \\ u_{rd} = p\psi_{rq} + \omega_1\psi_{sq} + R_{\mathrm{r}}i_{rq} \end{cases} \tag{1}$$

$$\begin{cases} \psi_{sd} = L_{\mathrm{s}}i_{sd} + L_{\mathrm{m}}i_{rd} \\ \psi_{sq} = L_{\mathrm{s}}i_{sq} + L_{\mathrm{m}}i_{rq} \\ \psi_{rd} = L_{\mathrm{r}}i_{rd} + L_{\mathrm{m}}i_{sd} \\ \psi_{rq} = L_{\mathrm{r}}i_{rd} + L_{\mathrm{m}}i_{sq} \end{cases} \tag{2}$$

where u_{sd}, u_{sq}, u_{rd}, and u_{rd} represent the stator and rotor voltage in d-q axis, respectively, and i_{sd}, and i_{sq}, and i_{rd}, and i_{rq} represent the stator and rotor current in d-q axis, respectively, and ψ_{sd}, ψ_{sq} represent the d-q axis component of the stator flux, respectively, and ψ_{rd}, ψ_{rq} represent the d-q axis component of the rotor flux, respectively, and p is the differential operator, and ω_1 is the angular frequency of power grid voltage.

The instantaneous active and reactive power of DFIG can be converted into a synchronously rotating d-q reference frame by

$$\begin{cases} P_{\mathrm{s}} = u_{sd}i_{sd} + u_{sq}i_{sq} \\ Q_{\mathrm{s}} = u_{sq}i_{sd} - u_{sd}i_{sq} \end{cases} \tag{3}$$

Let the d-axis be the direction of the stator flux vector, i.e. $\psi_{sd} = \psi_{\mathrm{s}}$, $\psi_{sq} = 0$, $u_{sd} = 0$, $u_{sq} = u_{\mathrm{s}}$. According to (1), (2) and (3), we obtain

$$\begin{cases} P_{\mathrm{s}} = u_{\mathrm{s}}i_{sq} = -\dfrac{u_{\mathrm{s}}L_{\mathrm{m}}}{L_{\mathrm{s}}}i_{rq} \\ Q_{\mathrm{s}} = u_{\mathrm{s}}i_{sd} = \dfrac{u_{\mathrm{s}}}{L_{\mathrm{s}}}(\psi_{\mathrm{s}} - L_{\mathrm{m}}i_{rd}) \end{cases} \tag{4}$$

From the above equations we can see that the power decoupling control can be easily achieved if i_{rd} and i_{rq} can be controlled, respectively. The simplified model given in the above equations is also used along with a controller to regulate the voltage at the power-grid connected point and control the power exchange.

3 Mathematical Model of STATCOM

STATCOM is a compensation device that is capable of generating or absorbing reactive power, and is made up of three components: voltage source converter (VSC), coupling transformer, and the control circuit[18]. The VSC is modelled as a six-pulse IGBT converter with a DC-link capacitor. The interaction between the AC system voltage and the STATCOM terminals voltage controls the reactive power flow. If the system voltage is higher than the voltage at the STATCOM terminals, the STATCOM behaves as an inductor and the reactive power transfers from the system to the STATCOM, and conversely. Under normal operating conditions, both voltages are equal and there is no power exchange between the STATCOM and the AC system. The

system topology configuration of STATCOM is show in Figure.2.

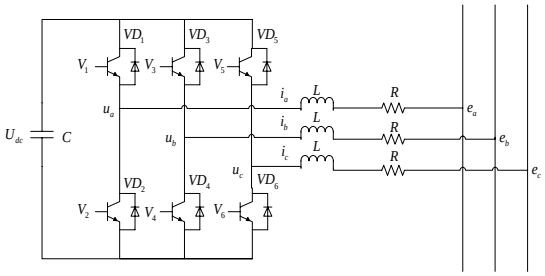

Fig.2 Circuit diagram of STATCOM

where i_a , i_b , i_c are the AC line currents of the STATCOM, and e_a , e_b , e_c are voltages of the point of common coupling(PCC), and u_a , u_b , u_c are the inverter terminal voltages, and R , L represent the equivalent conduction losses and the inductance for the transformer and filter, and U_{dc} is the voltage of DC capacitor.

To describe the STATCOM model more accurately, switching system is applied to reflect its work characteristics. In practice, STATCOM regulates the system bus voltage continuously by each switch state changing [15].

For an ideal switch S, if the switch turn-on is 1, and turn-off is 0, the switching function S can be then expressed by

$$S_j \in \{1,0\} \qquad j \in \{\mathrm{a},\mathrm{b},\mathrm{c}\} \tag{5}$$

Let us consider a three-phase balanced system of its parameters and voltages being symmetrical, the mathematical model of STATCOM can be represented by

$$\begin{cases} L\dfrac{di_a}{dt} = -Ri_a + e_a - S_a U_{dc} \\ L\dfrac{di_b}{dt} = -Ri_b + e_b - S_b U_{dc} \\ L\dfrac{di_c}{dt} = -Ri_c + e_c - S_c U_{dc} \end{cases} \tag{6}$$

Let ω be the angular frequency, through the Park transform, and then

$$\begin{bmatrix} i_d \\ i_q \end{bmatrix} = C \begin{bmatrix} i_a \\ i_b \\ i_c \end{bmatrix}$$

The transformation matrix C is described by

$$C = \sqrt{\frac{2}{3}} \begin{bmatrix} \cos\omega t & \cos(\omega t - \frac{2}{3}\pi) & \cos(\omega t + \frac{2}{3}\pi) \\ \sin\omega t & \sin(\omega t - \frac{2}{3}\pi) & \sin(\omega t + \frac{2}{3}\pi) \end{bmatrix} \tag{7}$$

We an then the general model on the *d*-*q* frame.

$$\begin{cases} L\dfrac{di_d}{dt} = -Ri_d + \omega L i_q + e_d - S_d U_{dc} \\ L\dfrac{di_q}{dt} = -Ri_q + \omega L i_d + e_q - S_q U_{dc} \end{cases} \tag{8}$$

where the physical meaning of the variables with subscript d and q correspond to one of subscript a, b, and c in (6), which are the transformed result from the three-phase modulating signals to the two.

From the above equations, the control of bus voltage and the current generated by wind farms should be selected as the control variables. Therefore, the STATCOM subsystem is a strongly coupled system with two degree of control freedom.

However, under the condition of an unbalanced voltage system, the mathematical model of STATCOM should be re-established.

Because of the three-phase unbalanced system with no neutral point connection, the zero-sequence is neglected. As a result, the output voltage of STATCOM consists of positive and negative sequence which can be converted into a synchronously rotating *d*-*q* reference frame. According to the theory of symmetric component, the positive coordinate system rotates counter clockwise whereas the negative rotates clockwise. Each coordinate vector diagram is shown in Figure 3.

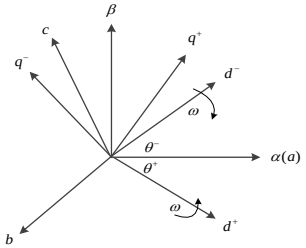

Fig.3 Coordinate vector diagram

In Figure3, the three-phase static coordinate system is presented by abc , and $\alpha\beta$ is the two-phase static coordinate system, and d^+ , q^+ are the two-phase rotary positive coordinate system, and d^- , q^- are the two-phase rotary negative coordinate system, and θ^+ , θ^- are the angle between $\alpha\beta$ and dq , and ω is the angular velocity.

Through the transformation matrix C^+ and C^-, the three-phase static coordinate system abc can be converted into two-phase static coordinate one $\alpha\beta$, and then it is changed into two-phase rotary coordinate system dq. C^+, C^- can be written by

$$C^+ = \sqrt{\frac{2}{3}}\begin{bmatrix} \cos\omega t & \cos(\omega t-\frac{2}{3}\pi) & \cos(\omega t+\frac{2}{3}\pi) \\ -\sin\omega t & -\sin(\omega t-\frac{2}{3}\pi) & -\sin(\omega t+\frac{2}{3}\pi) \end{bmatrix}$$

$$C^- = \sqrt{\frac{2}{3}}\begin{bmatrix} \cos\omega t & \cos(\omega t+\frac{2}{3}\pi) & \cos(\omega t-\frac{2}{3}\pi) \\ \sin\omega t & \sin(\omega t+\frac{2}{3}\pi) & \sin(\omega t-\frac{2}{3}\pi) \end{bmatrix}$$

After Park-Clarke transformation, we get the mathematical model of STATCOM on the d^+, q^+ and d^-, q^- frame below.

$$\begin{cases} L\dfrac{di_d^+}{dt} = -Ri_d^+ + \omega Li_q^+ + e_d^+ - S_d^+U_{dc} \\ L\dfrac{di_q^+}{dt} = -Ri_q^+ - \omega Li_d^+ + e_q^+ - S_q^+U_{dc} \end{cases} \tag{9}$$

$$\begin{cases} L\dfrac{di_d^-}{dt} = -Ri_d^- - \omega Li_q^- + e_d^- - S_d^-U_{dc} \\ L\dfrac{di_q^-}{dt} = -Ri_q^- - \omega Li_d^- + e_q^- - S_q^-U_{dc} \end{cases} \tag{10}$$

where i_d^+, i_q^+, e_d^+, e_q^+ are the currents and voltages of positive sequence coordinate, respectively, and i_d^-, i_q^-, e_d^-, e_q^- are the currents and voltages under negative sequence coordinate, respectively, and S_d^+, S_q^+, S_d^-, S_q^- are the switch function of positive and negative coordinate, respectively.

Therefore, the STATCOM subsystem can transform a strongly coupled plant with two degrees of control freedom into independent control of positive and negative component.

4 Reactive Current Detection Method of STATCOM

According to the work principle of STATCOM, it is of significance to detect the fundamental reactive current rapidly and accurately. Due to $p-q$ and i_p-i_q current detection method based on instantaneous reactive power theory that will produce detecting error in case of three-phase asymmetrical systems, the synchronous rotation angle not can track the changes of grid voltage fundamental positive frequency in real time so that the traditional i_p-i_q method will produce errors.

4.1 Traditional i_d-i_q detection method

Three-phase asymmetrical voltages and currents can be described by

$$\begin{bmatrix} u_a \\ u_b \\ u_c \end{bmatrix} = \begin{bmatrix} \sqrt{2}\sum_{n=1}^{\infty}[U_{n+}\sin(n\omega t+\varphi_{n+}) + \\ U_{n-}\sin(n\omega t+\varphi_{n-}) + u_0] \\ \sqrt{2}\sum_{n=1}^{\infty}[U_{n+}\sin(n\omega t-\frac{2}{3}\pi+\varphi_{n+}) + \\ U_{n-}\sin(n\omega t+\frac{2}{3}\pi+\varphi_{n-}) + u_0] \\ \sqrt{2}\sum_{n=1}^{\infty}[U_{n+}\sin(n\omega t+\frac{2}{3}\pi+\varphi_{n+}) + \\ U_{n-}\sin(n\omega t-\frac{2}{3}\pi\text{-}\varphi_{n-}) + u_0] \end{bmatrix}$$

$$\begin{bmatrix} i_a \\ i_b \\ i_c \end{bmatrix} = \begin{bmatrix} \sqrt{2}\sum_{n=1}^{\infty}[I_{n+}\sin(n\omega t+\varphi'_{n+}) + \\ I_{n-}\sin(n\omega t+\varphi'_{n-}) + i_0] \\ \sqrt{2}\sum_{n=1}^{\infty}[I_{n+}\sin(n\omega t-\frac{2}{3}\pi+\varphi'_{n+}) + \\ I_{n-}\sin(n\omega t+\frac{2}{3}\pi+\varphi'_{n-}) + i_0] \\ \sqrt{2}\sum_{n=1}^{\infty}[I_{n+}\sin(n\omega t+\frac{2}{3}\pi+\varphi'_{n+}) + \\ I_{n-}\sin(n\omega t-\frac{2}{3}\pi+\varphi'_{n-}) + i_0] \end{bmatrix}$$

where u_a, u_b, u_c and i_a, i_b, i_c are the instantaneous values of asymmetrical voltages and currents, respectively, and U_n, I_n are the effective value of asymmetrical voltages and currents, and n is harmonic order, and φ_n is initial phase angle of voltage, and φ'_n is initial phase angle of current, where subscript "+", "−", "0" denote positive, negative and zero sequence, respectively.

In condition of asymmetrical voltage, the phase difference θ between phase angle of u_a and one of actual voltage fundamental positive sequence can be generated by phase locked loop (PLL), which is needed in process of the rotation transformation.

The transformation matrix from three-phase static coordinate to two-phase rotating coordinate is then described by

$$C_{dq}=\sqrt{\frac{2}{3}}\begin{bmatrix}\cos(\omega t+\theta) & \cos(\omega t-\frac{2}{3}\pi+\theta) & \cos(\omega t+\frac{2}{3}\pi+\theta)\\ \sin(\omega t+\theta) & \sin(\omega t-\frac{2}{3}\pi+\theta) & \sin(\omega t+\frac{2}{3}\pi+\theta)\end{bmatrix}$$

Conducting the *d-q* transform from u_a, u_b, u_c, and i_a, i_b, i_c, and we then obtain

$$\begin{bmatrix}u_d\\ u_q\end{bmatrix}=C_{dq}\begin{bmatrix}u_a\\ u_b\\ u_c\end{bmatrix}\qquad\begin{bmatrix}i_d\\ i_q\end{bmatrix}=C_{dq}\begin{bmatrix}i_a\\ i_b\\ i_c\end{bmatrix}$$

After low-pass filter (LPF), we obtain

$$\begin{bmatrix}\overline{u_d}\\ \overline{u_q}\end{bmatrix}=\begin{bmatrix}\sqrt{3}U_{1+}\cos(\varphi_{1+}-\theta)\\ \sqrt{3}U_{1+}\sin(\varphi_{1+}-\theta)\end{bmatrix}\tag{11}$$

$$\begin{bmatrix}\overline{i_d}\\ \overline{i_q}\end{bmatrix}=\begin{bmatrix}\sqrt{3}I_{1+}\cos(\varphi_{1+}-\theta)\\ \sqrt{3}I_{1+}\sin(\varphi_{1+}-\theta)\end{bmatrix}\tag{12}$$

where $\overline{u_d}$, $\overline{u_q}$ and $\overline{i_d}$, $\overline{i_q}$ are dc components of u_d, u_q and i_d, i_q, respectively. And U_{1+}, I_{1+} are the effective values of fundamental positive voltage and current.

Obviously, the calculation result is not accurate since there is phase angle difference between actual voltage and its positive sequence voltage.

4.2 Improved $i_d - i_q$ detection method

Under condition of asymmetrical voltage, an improved detection method is proposed and vector diagram is shown in Figure.4.

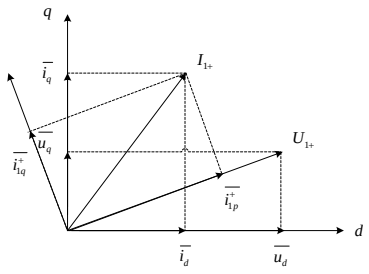

Fig.4 Vector diagram of fundamental positive sequence voltage and current

In Figure 4, $\overline{i_{1p}^+}$ and $\overline{i_{1q}^+}$ separately express the actual fundamental positive active and reactive current. Seen from Fig.4, $\overline{i_{1p}^+}\neq\overline{i_d}$, and $\overline{i_{1q}^+}\neq\overline{i_q}$, and so there exists a principle error. Below we try then to eliminate the detection errors.

The instantaneous fundamental active power can be shown by

$$\overline{p}=\overline{u_d}\,\overline{i_d}+\overline{u_q}\,\overline{i_q}\tag{13}$$

Then

$$\overline{i_{1p}^+}=\frac{\overline{p}}{\sqrt{\overline{u_d}^2+\overline{u_q}^2}}\tag{14}$$

And phase difference α between U_{1+} and d - axis can be described by

$$\cos\alpha=\frac{\overline{u_d}}{\sqrt{\overline{u_d}^2+\overline{u_q}^2}}\qquad\sin\alpha=\frac{\overline{u_q}}{\sqrt{\overline{u_d}^2+\overline{u_q}^2}}$$

And then active and reactive component of fundamental positive current can be obtained by

$$\overline{i_{d,1p}^+}=\frac{\overline{u_d}}{\overline{u_d}^2+\overline{u_q}^2}(\overline{u_d}\,\overline{i_d}+\overline{u_q}\,\overline{i_q})\tag{15}$$

$$\overline{i_{q,1p}^+}=\frac{\overline{u_q}}{\overline{u_d}^2+\overline{u_q}^2}(\overline{u_d}\,\overline{i_d}+\overline{u_q}\,\overline{i_q})\tag{16}$$

Based on the detection method of dynamic active and reactive current analyzed above, the actual three-phase active component of fundamental positive sequence current $i_{a,1p}^+$, $i_{b,1p}^+$, $i_{c,1p}^+$ can be worked out, and then subtracted using the three-phase current i_a, i_b, and i_c, respectively. The compensation commending current can be then acquired as i_a^*, i_b^*, i_c^*. Thus, the error is then eliminated.

Hence, the improved detection method schematic diagram is shown in Figure 5.

Active and reactive component of fundamental positive current can be obtained correctly through the above method regardless of the asymmetrical condition, which is more accurate than tradition ones.

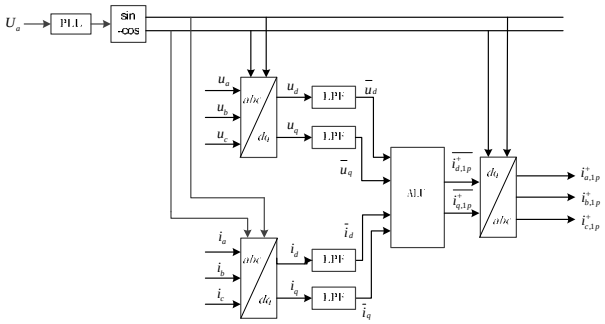

Fig.5 Schematic diagram of an improved $i_d - i_q$ detection method

5 Simulation Analysis

The single line diagram of the power grid used for this investigation is illustrated in Figure 6. The grid model consists of a 25kV grid, feeding a 575V system through 575V/25kV step-up transformer. The DFIG based wind farm of a protection system to monitor voltage, current, machine speed and DC link voltage is connected at 575V bus. The 3Mvar STATCOM is shunt connected at the sending end 25kV bus to provide dynamic compensation of reactive power. In this simulation, the diode rectifier bridge with inductive load is employed on grid side.

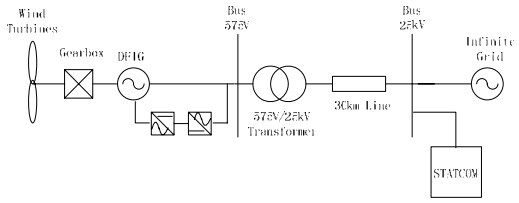

Fig.6 Single Line Diagram of Power Grid System

The main parameters of the generator system in Figure 6 are given in Table 1.

Tab.1 The parameters of system

u_s	L_s	L_r	L_m	R_s	R_r
575	0.171	0.156	2.9	0.00706	0.005

In order to verify the correctness and effectiveness of detection method presented in this paper, the wind power system based on STATCOM system shown in Figure 6 is simulated in Matlab simulation environment.

The simplified equivalent circuit of system is shown in Figure.7.

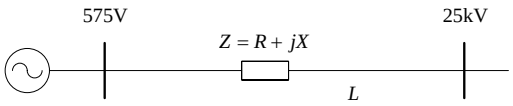

Fig.7 Simplified equivalent circuit of system

The parameters of the simplified equivalent circuit is R, X and L. And $R = 0.1153\Omega/\text{km}$, $X = 0.00332\text{H}/\text{km}$ and $L = 30\text{km}$.

The real and reactive power Q_c injected by the STATCOM is given by following equation

$$\Delta U = \frac{P_s R + (Q_s - Q_c)X}{U} \tag{17}$$

where ΔU is the value of voltage sag, U is the bus voltage.

Grid fault has a significant effect on the wind farm, and it is simulated starting at t=1s and lasts for 0.2s, the impact of this asymmetrical fault on the performance of the STATCOM is discussed below.

5.1 One-phase-ground fault

To verify the effectiveness of the proposed method, one-phase-ground fault of the 25kV-bus AC system has been simulated. The fault features of the three-phase positive sequence voltage, the active and reactive power of system are shown in Figure.8 to Figure.10.

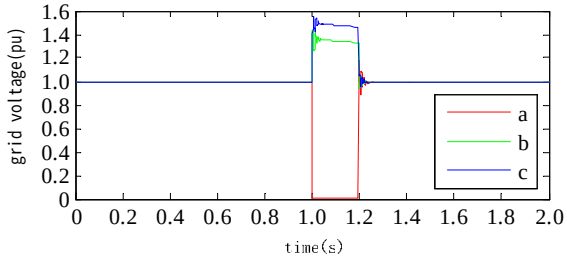

Fig.8 Waveform of grid voltage under fault

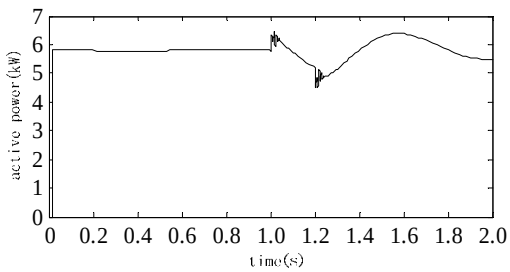

Fig.9 Waveform of active power of grid

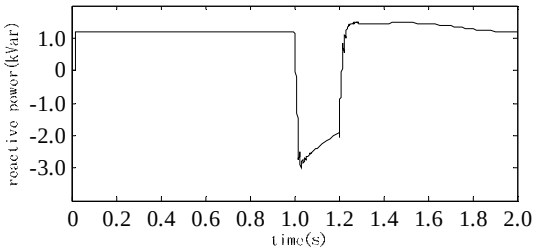

Fig.10 Waveform of reactive power of grid

Fig.8 shows the three phase positive sequence voltage of grid side, and Fig.9 shows the active power of grid, and Fig.10 shows the reactive power of grid.

Figure.11 shows that the DFIG terminal voltage experiences voltage sag of 78% of its nominal value during the one-phase-ground grid fault, and the generator voltage can be recovered after fault clearance.

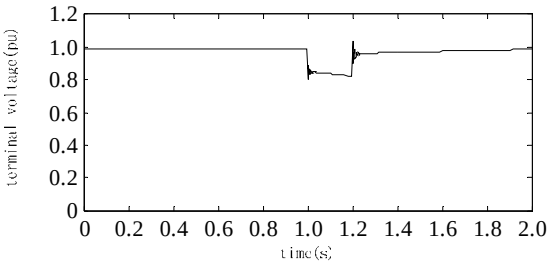

Fig.11 Waveform of terminal voltage

When the STATCOM is connected, the proposed detection method of either the traditional or improved method in controller acts immediately to inject reactive power to the grid during the fault, and the waveform of terminal voltage are rectified shown in Figure 12 and Figure 13, wherein Figure.12 represents the traditional detection method and Figure.13 represents the improved detection method.

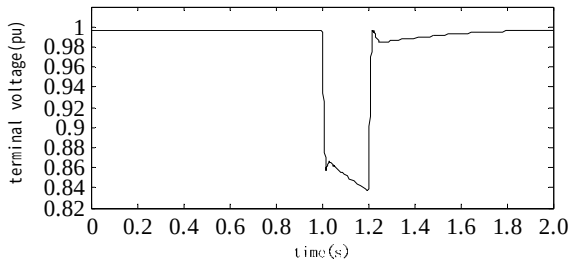

Fig.12 Waveform of traditional detection method

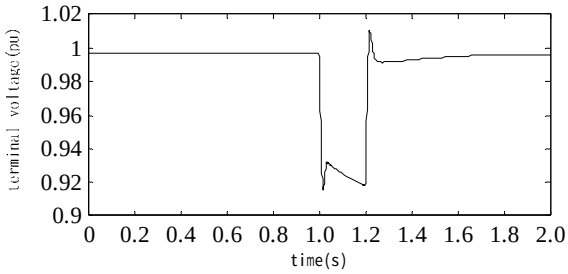

Fig.13 Waveform of improved detection method

Seen from Fig.12 and Fig.13, the terminal voltage is improved to 86% using traditional detection method whereas to 92% is the improved method mentioned in this paper. Comparison results demonstrate that the improved detection method is more effective.

5.2 Two-phase-ground fault

Two-phase-ground fault also has been simulated in grid side. The fault features of the three-phase positive sequence voltage, active and reactive power of system are shown in Fig.14 to Fig.16.

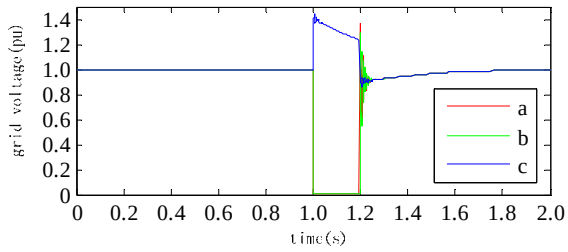

Fig.14 Waveform of two-phase-ground fault

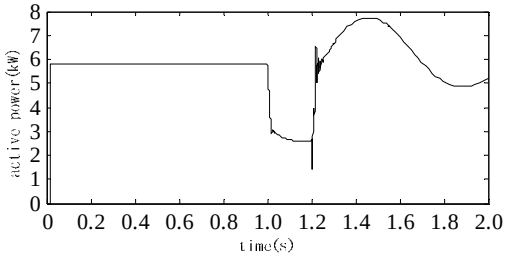

Fig.15 Waveform of active power of grid

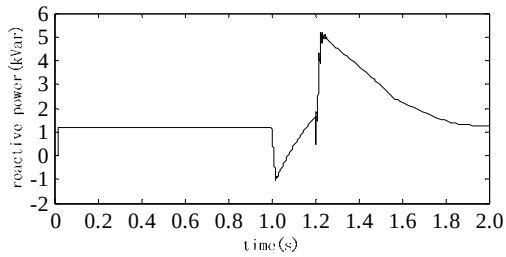

Fig.16 Waveform of reactive power of grid

Fig.14 shows the three phase positive sequence voltage of grid side with a phase and b phase grounding. Fig.15 shows the active power of grid. Fig.16 shows the reactive power of grid.

Figure.17 shows that the DFIG terminal voltage experiences voltage sag of 52% under the condition of two-phase ground fault.

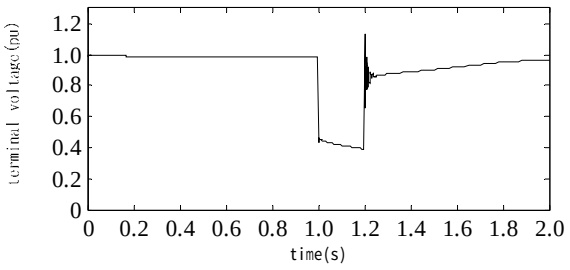

Fig.17 Waveform of terminal voltage

The proposed detection method of either the traditional or improved method acts immediately to inject reactive power to the grid during two-phase-ground fault and the waveform of terminal voltage is rectified shown as Figure.18 and Figure.19, wherein Figure.18 represents the traditional detection method and Figure.19 represents the improved detection method.

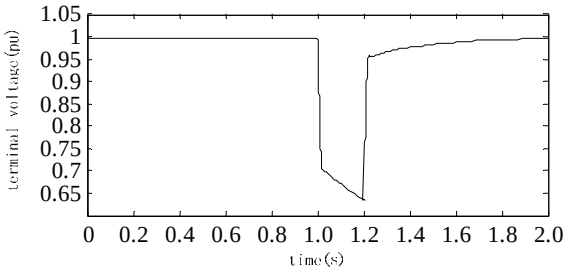

Fig.18 Waveform of traditional detection method

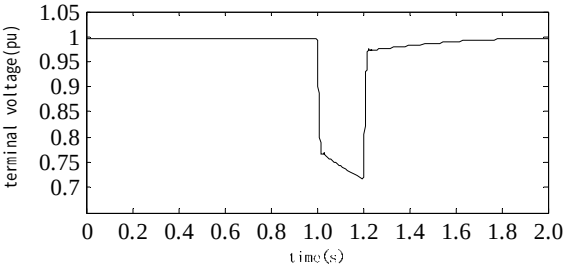

Fig.19 Waveform of improved detection method

We can see from Fig.18 and Fig.19 that the terminal voltage is improved to 68% using traditional detection method whereas 76% is the improved detection method. Comparison results show that the proposed method is more effective.

Comparison results under different faults show that when the grid faults occur at the same location, one-phase-ground leads to the slighter positive sequence voltage sags than two-phase-ground fault, and we can also see that the terminals voltage of DFIG is immediately rectified using the mentioned $i_d - i_q$ detection method.

6 Conclusions

This paper proposes an improved detection method of fundamental positive current under grid-side asymmetrical faults. Compared with traditional detection method, the presented method compensates the deficiencies that there are detecting errors existing in traditional ones aroused by asymmetrical faults, and that makes the STATCOM work more effective. This is quite significant for safe operation of the wind power plant grid-connected. But before that, more detailed model and control of the system should be examined, the system behaviour and its control under other fault condition, which will be included in our future work.

References:

[1] Xu Wang, Yi Liu, Na Jiang, Summary of wind power technology development, *Electric switchgear*, Vol.3, 2013, pp.16-19.

[2] Qiuming Chen, Hongmei Li, Comparison between two main wind power generators, *Dongfang electric review*, Vol. 24, No.93, 2010, pp.41-44.

[3] Lin Zhang, Weidong Qiu, Consideration of large-scale wind farm disconnection from grid, *Electric power construction*,Vol.33, No.3, 2010, pp.11-14.

[4] Z. Chen and E. Spooner, Grid power quantity with variable speed wind turbines. *Energy Conversation, IEEE Transactions on*, Vol.16, 2001, pp.148-154.

[5] M. J. Ghorbanifar, J. Ahmadian, S. Shams, F. Goodarzvand, Overview of grid connected doubly-fed induction generator power quantity, *In Clean Energy and Technology (CEAT), 2013 IEEE conference on*, 2013, pp.146-151.

[6] H. Chaal and M. Jovanovic, Toward a Generic Torque and Reactive Power Controller for Doubly Fed Machines, *Power Electronics, IEEE Transactions on*, Vol. 27, 2012, pp.113-121.

[7] Chao Li, Research on problems of STATCOM to improve voltage stability of wind farms, *Tianjin University*, Tianjin, China, 2013.

[8] Lee C K, Leung, J S K, S Y R, et al, Circuit-level companions of STATCOM technologies, *IEEE Trans on power Electronics*, Vol. 18, No.4, 2003, pp.1084-1092.

[9] Jixin Zhu, Application of 50Mvar STATCOM in shanghai power grid, *Electric power construction*, Vol. 27, No.12, 2006, pp.14-17.

[10] Liang Liu, Minggao Deng, Honglin Ouyang, A research of adaptive detection algorithm for D-STATCOM, *Power System Protection and control*, Vol.39, No.5, 2011, pp.115-119.

[11] Herrera R S, Instantaneous reactive power theory: a reference in the nonlinear loads compensation, *IEEE Trans on Industrial Electronics*，Vol.56, No.6, 2009, pp. 2015-2022.

[12] Lei Tang, Weirong Chen, Deduction of coordinate transform for instantaneous reactive power theory and analysis on the principle of harmonic current detection method, *Power System Technology*, Vol.32, No.5, 2008, pp.66-69.

[13] Ekanayake J B, Hold worth L and Wu X G. Dynamic modeling of doubly-fed induction generator wind turbines, *Power system*, Vol.12, No.8, 2003, pp.803-809.

[14] Shengzhou Dong, and R spee, Synchronous frame model and decoupled control developed for doubly-fed machines, *Proceedings of IEEE industry electronics specialist conference*, 1994, pp.1229-1236.

[15] Houjian Zhan, Jiekang Wu, Haibing Kang, The switching function modeling and simulation of STATCOM, *Power system protection and control*, Vol.38, No.10, 2010, pp.66-70.

[16] A. S. Oshaba, and E. S. Ali, "Speed Control of Induction Motor Fed from Wind Turbine via Particle Swarm Optimization Based PI Controller", Research Journal of Applied Sciences, Engineering and Technology, (Maxwell Science Publication), Vol. 5, No. 18, May 2013, pp. 4594-4606.

[17] E. S. Ali, "Speed Control of Induction Motor Supplied by Wind Turbine via Imperialist Competitive Algorithm", Energy (Elsevier), Vol. 89, September 2015, pp. 593-600.

[18] S. M. Abd-Elazim, and E. S. Ali, "Imperialist Competitive Algorithm for Optimal STATCOM Design in a Multimachine Power System", Int. J. of Electrical Power and Energy Systems (IJEPES Elsevier), Vol. 76 C, March 2016, pp. 136-146.